

Effect of Ladle Changeover Condition on Transient Three-Phase Flow in a Five-Strand Bloom Casting Tundish



HUA ZHANG, QING FANG, RONGHUA LUO, CHAO LIU, YI WANG,
and HONGWEI NI

The transient three-phase flow behavior in a five-strand bloom casting tundish during the ladle changeover process considering a constant casting speed was investigated by the VOF model, and the effect of ladle throughput rate, shroud immersion depth, turbulence inhibitor structure and ladle changeover time on the turbulent flow, and level fluctuations during the filling process were analyzed to optimize the flow pattern in the tundish during ladle changeover. The results showed that the exposed area of molten steel in the impact zone increases as the ladle throughput rate increases during the filling process and that the exposure of molten steel is eliminated when the ladle throughput rate is $1.5Q_{\text{steady}}$. As the immersion depth of the shroud increases, a slight decrease in slag entrainment happens, while the exposed area of molten steel first decreases and then increases. The shroud immersion depth should be 310 mm. When the optimized turbulence inhibitor is used, the wave crests of the steel level are greatly reduced, the height of the level fluctuation is alleviated with the maximum value decreasing from 33 mm to approximately 10 mm, and the exposure of molten steel is eliminated. When the ladle changeover time is between 2 and 3 minutes, the exposed area of molten steel during the stable period of the filling process is in the range from 150 to 170 cm², which is substantially less than the exposed area of 500 cm² when the ladle changeover time is 4 minutes. Therefore, the ladle changeover time should be controlled within 3 minutes. The flaw detection disqualification rate caused by ladle changeover operation is decreased from 43.8 to 25.8 pct of the total disqualified steel rails after optimization.

<https://doi.org/10.1007/s11663-019-01572-6>

© The Minerals, Metals & Materials Society and ASM International 2019

I. INTRODUCTION

IT is well known that the flow behavior in a bloom casting tundish is very important for the quality of the bloom and that many defects in the steel products are induced by entrapment of slag and reoxidation of steel in the tundish.^[1,2] There are two stages in tundish metallurgy: the steady-state operation and the transient casting operation. A large number of papers published during the last decade, even recently, have focused on modeling the residence time distribution (RTD), multiphase flow, nonmetallic inclusion

behavior, and heat loss, among others, during the steady-state operation period of tundish metallurgy, predominantly by homogeneous turbulent flow models.^[3-6]

Transient-state operations in a tundish, such as the start-up, ladle changeover, and end of sequence processes,^[7] are the main determining factors affecting the stability and purity of the molten steel injected into the mold. Comparatively, the two- and three-phase modeling of the transient casting process has been less thorough and relatively rare. Modeling the transient multiphase turbulent flow behavior in the tundish is a relatively difficult task with complicated metallurgical behaviors and needs large calculation resources, especially for the ladle changeover process. Fernandez Oro *et al.*^[8] and Jha *et al.*^[9,10] paid attention to the variation in steel intermixed concentration with the filling time and under different casting conditions, while the liquid level fluctuation and the steel–slag–gas three-phase behaviors were ignored. Takahashi *et al.*^[11] investigated the velocity field during ladle changeover and proposed a rule to predict the floating condition of nonmetallic inclusions. Lin *et al.*^[12-14] investigated the steel flow, heat loss, and removal behavior of nonmetallic inclusions in a 2-strand

HUA ZHANG, QING FANG, CHAO LIU, YI WANG, and HONGWEI NI are with the State Key Laboratory of Refractories and Metallurgy, Wuhan University of Science and Technology, No. 947, Heping Avenue, Qingshan District, Wuhan, 430081, P.R. China and also with the Key Laboratory for Ferrous Metallurgy and Resources Utilization of Ministry of Education, Wuhan University of Science and Technology. Contact e-mails: qingfang@wust.edu.cn, nihongwei@wust.edu.cn RONGHUA LUO is with the Valin Xiangtan Iron and Steel Co., Ltd., Xiangtan, 411101, P.R. China.

Manuscript submitted November 8, 2018.

Article published online April 12, 2019.

tundish in the steady and transient states and analyzed the effects of the operations of sudden stopping, ladle changeover, and sudden closing of one strand on the cleanliness of molten steel. However, the behaviors of level fluctuations and slag entrapment, which also significantly affect the cleaning of liquid steel during these operations, were ignored. Despite the importance of transient operations to steel quality, few studies dealing with the tundish filling process during ladle changeover consider the effect of the large increase in the injection velocity on level fluctuations, the change in steel level, and slag and air entrapment during ladle changeover operations. Morales *et al.*^[15,16] developed a transient, three-phase, turbulent volume of fluid (VOF) model to investigate slag entrainment during ladle changeover operation in a single-strand tundish under different shroud structures and demonstrated that the dissipative ladle shroud (LS) can substitute turbulent control devices to improve the fluid behavior during ladle changeover and can efficiently reduce the chance of slag and air entrapment. However, their model focused on only the flow behavior of water and oil and did not encompass all the characteristic features of industrial ladle changeover processes. Moreover, tundish designs (turbulence inhibitor, shroud structure, *etc.*) and methods of controlling casting conditions (ladle throughput rate, immersion depth of LS, ladle changeover time, *etc.*) that are intended to improve the ladle changeover behaviors instead of controlling only the steady operation and to enable the study of real turbulent flows in the tundish during these transient periods are rarely reported today. Moreover, most of the existing contributions about the ladle changeover process are concentrated on the metallurgical behavior in the entire tundish, while the exact effect of ladle changeover conditions on turbulent behaviors in the impact zone remains to be thoroughly investigated.

The five-strand continuous casting bloom produced in a specific steelmaking plant is mainly used for producing high rails. In this plant, 368 of 28,850 steels rails produced in three months were disqualified because of flaw detection, and 161 of the 368 rails (approximately 43.8 pct) were rolled from the blooms produced during ladle changeover. Therefore, in this contribution, the three-dimensional multiphase (air–slag–steel) flow behaviors in a five-strand bloom casting tundish during the ladle changeover process were simulated by the VOF model, in which the level change in liquid steel and a constant casting speed during the ladle changeover operation were considered. Water model experiments were conducted to validate the simulated results of level fluctuations and the exposed area of molten steel. The effects of ladle throughput rate, shroud immersion depth, turbulence inhibitor structure, and ladle changeover time on the level fluctuations, slag and air entrapment, and exposed area of molten steel during the filling process of the ladle changeover operation were also investigated and compared to further improve the flow pattern and steel cleanliness in the bloom casting tundish during ladle changeover. Moreover, the optimized ladle changeover conditions were applied in industrial trials for three months, and the flaw detection results of the steel rails produced before and after optimization were compared.

II. MODEL DESCRIPTIONS

A. Basic Assumptions

The basic assumptions for modeling the transient multiphase flow in the five-strand tundish during ladle changeover are as follows:

1. There is no chemical interaction among the three kinds of fluids in the tundish during the pouring process.
2. Only the liquid-state cover slag is considered in the calculations.
3. The three phases (steel, slag, and air) are treated as incompressible Newtonian fluids with fixed physical properties.
4. The effect of temperature change on the flow pattern of the fluids in the tundish is ignored.

B. Governing Equations

1. Fundamental equations

Three-dimensional continuity and the Navier–Stokes equations are shown as follows, together with the standard k- ε model:

$$\nabla \cdot (\rho_m \vec{v}_m) + \frac{\partial \rho_m}{\partial t} = 0, \quad [1]$$

$$\frac{\partial (\rho_m \vec{v}_m)}{\partial t} + \nabla \cdot (\rho_m \vec{v}_m \vec{v}_m) = -\nabla p + \mu_m \nabla^2 \vec{v}_m + \rho_m \vec{g}, \quad [2]$$

where \vec{v}_m is the mixture velocity; ρ_m and μ_m are the density and viscosity of fluid; and p is the pressure.

2. Turbulent model

The turbulent behavior in the tundish during the ladle changeover process is expressed by the standard k- ε model^[17,18]:

$$\frac{\partial (\rho_m k)}{\partial t} + \nabla \cdot (\rho_m \vec{v}_m k) = \nabla \cdot \left[\left(\mu + \frac{\mu_{t,m}}{\sigma_k} \right) \nabla k \right] + G_k - \rho_m \varepsilon, \quad [3]$$

$$\frac{\partial (\rho_m \varepsilon)}{\partial t} + \nabla \cdot (\rho_m \vec{v}_m \varepsilon) = \nabla \cdot \left[\left(\mu + \frac{\mu_{t,m}}{\sigma_k} \right) \nabla \varepsilon \right] + C_{1\varepsilon} \frac{\varepsilon}{k} G_k - C_{2\varepsilon} \rho_m \frac{\varepsilon^2}{k}, \quad [4]$$

where G_k represents the generation of turbulence kinetic energy due to the mean velocity gradients, the turbulent viscosity $\mu_{t,m}$ and effective viscosity μ_m are calculated by

$$\mu_m = \mu_{t,m} + \mu, \mu_{t,m} = \rho_m c_\mu k^2 / \varepsilon, \quad [5]$$

where the values of model constants $C_{1\varepsilon}$, $C_{2\varepsilon}$, c_μ , σ_k , and σ_ε are 1.43, 1.92, 0.09, 1.0, and 1.3, respectively.

3. VOF model

To accurately simulate the dynamic behavior of the three-phase flow in the tundish during ladle changeover, the VOF model is applied to investigate the behavior of steel–slag–air interfaces. The tracking of the interfaces between the phases is accomplished by the solution of a continuity equation for the volume fraction of one (or more) of the phases. For the i th phase, this equation has the following form:

$$\frac{1}{\rho_i} \left[\frac{\partial}{\partial t} (\alpha_i \rho_i) + \nabla \cdot (\alpha_i \rho_i \vec{v}_m) \right] = S_{\alpha_i} + \sum_{i=1}^n (m_{ij}^{\rightarrow} - m_{ji}^{\rightarrow}) \quad [6]$$

where m_{ij}^{\rightarrow} and m_{ji}^{\rightarrow} are the mass of phase i flowing into phase j and phase j flowing into phase i , respectively; \vec{v}_m is the mixture velocity; α_i represents the volume fraction of phase i in the control cell; ρ_i is the density of phase i ; and the source term on the right-hand side of the equation (S_{α_i}) is zero. The volume fractions of all phases sum to unity in each control volume:

$$\sum_{i=1}^n \alpha_i = 1. \quad [7]$$

A single momentum equation is solved throughout the domain, and the resulting velocity field is shared among the phases, which is shown as follows:

$$\frac{\partial(\rho_m \vec{v}_m)}{\partial t} + \nabla \cdot (\rho_m \vec{v}_m \vec{v}_m) = -\nabla p + \nabla [\mu(\nabla \vec{v}_m + \nabla \vec{v}_m^T)] + \rho_m \vec{g} + \vec{F}. \quad [8]$$

The averaged thermal physical properties in the cell are applied in the calculations, such as density (ρ_m)

$$\rho_m = \sum_{i=1}^n \alpha_i \rho_i. \quad [9]$$

The surface tension can be written in terms of the pressure jump across the surface. The force at the surface can be expressed as a volume force using the divergence theorem. It is this volume force that is the source term that is added to the momentum equation. It has the following form: \vec{F} is the surface tension force item:

$$\vec{F} = \sum_{\text{parisij}, i < j}^3 \frac{2\sigma_{ij} \alpha_i \rho_i k_j \nabla \alpha_j + \alpha_j \rho_j k_i \nabla \alpha_i}{\rho_i + \rho_j}, \quad [10]$$

where σ_{ij} is interfacial tension among phases i and j , and k_i and k_j are their radiuses of curvature. The interfacial surface tensions were calculated knowing the surface tension of phase i and j through following equation:

$$\sigma_{ij} = (\sigma_i^2 + \sigma_j^2 - 2\sigma_i \sigma_j \cos \theta)^{\frac{1}{2}}, \quad [11]$$

where σ_i and σ_j are the surface tension of phase i and j , respectively; θ is the contact angle between phase i and j .

4. Initial and boundary conditions

The transient casting process in the tundish during ladle changeover can be divided into two stages (Figure 1). One is the closure of the shroud, during which the level of the steel drawdown drops due to the constant outflow of steel into submerged entry nozzles (SEN); the other stage is the reopening of shroud, which causes the level of the fluids to rise as the injection rate of molten steel from the ladle to the tundish becomes higher than the outflow rate. The W_{tundish} and Q_{steady} in Figure 1 are the weight of molten steel in the tundish and the injection rate of molten steel at steady state. Figure 1 also shows that the injection rate of molten steel during the second step of the ladle changeover process is twice Q_{steady} and that the filling process takes 3 minutes. When the level of molten steel reaches the steady state, the injection rate returns to Q_{steady} .

The boundary conditions for the calculations can be set as follows based on the flow characteristics in the tundish:

1. Computational inlet: The velocity inlet boundary condition is applied for the filling process. The turbulent kinetic energy $k = 0.01 u_{\text{inlet}}^2$ and turbulent dissipation rate $\varepsilon = 2k^{1.5}/d_{\text{inlet}}$ are obtained with an empirical formula, where u_{inlet} and d_{inlet} are the velocity and equivalent diameter at the shroud inlet, respectively.
2. Considering a constant casting speed during the whole casting process, the velocity of the computational outlet is set to a constant value during the ladle changeover process. The velocity can be calculated from a cross section of the bloom and SEN and the casting speed.
3. The pressure inlet boundary is applied for the top surface of the tundish, and the value should be at standard atmospheric pressure.
4. The horizontal gradients for all variables at the symmetry plane are set to zero.

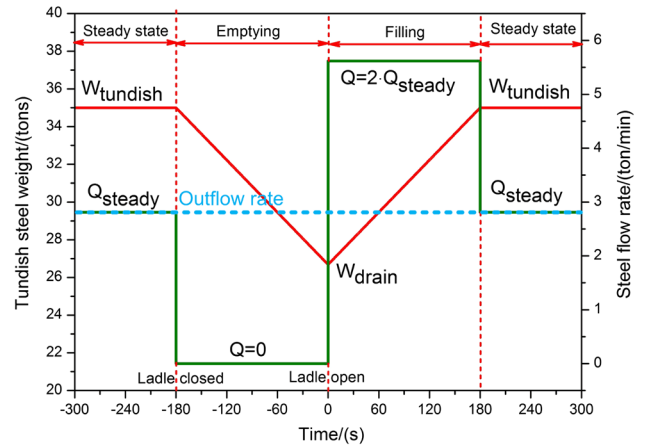


Fig. 1—Process diagram during ladle changeover in the tundish.

C. Computational Model

A three-dimensional mathematical multiphase model is developed based on the real size of an industrial tundish, and a schematic view and the dimensions of the industrial tundish are shown in Figure 2(a). To enhance the calculation efficiency and ensure accuracy, half of the real tundish is taken as the computational domain considering the symmetry of the tundish. The mesh distribution of the computational model is presented in Figure 2(b). To more accurately simulate the behavior of the steel–slag–air interface and impact zone of the tundish, local grid refinement technology is applied in the computational domain, the mesh around the steel–slag interface zone is refined, and the total number of meshed cells in the computational domain is approximately 1,000,000. Moreover, the main industrial conditions of the continuous casting tundish are presented in Table I.

The mathematical model is solved by the computational fluid dynamic software FLUENT 14.5. The pressure implicit with splitting of operators (PISO) algorithm is chosen for coupling the pressure and velocity terms, and the convergence criterion for each calculation is established when the value of all residuals for the dependent variable is under 10^{-4} . Moreover, under-relaxation factors for the moment, pressure, turbulent kinetic energy, turbulent dissipation rate, and turbulent viscosity are set to 0.3, 0.2, 0.15, 0.15, and 0.2, respectively, with a time step of 0.002 seconds to enhance the convergence history. The densities of molten steel, slag, and air used in the calculations are

7020, 2700, and 1.225 kg/m^3 , respectively, and the corresponding viscosities are 0.0062, 0.2 Pa s, and $1.79 \times 10^{-5} \text{ Pa s}$.

The geometric reconstruction approach^[18] is applied to obtain the face fluxes for a cell near the interface between two phases whenever the cell is completely filled with one phase or another. In this approach, the interface between fluids is represented through a piecewise-linear approach, which assumes that the interface has a linear slope within each cell, and uses this linear shape for the calculation of the advection of fluid through the cell faces.

III. RESULTS AND DISCUSSIONS

A. Model Validations

The simulation results of the multiphase flow field are verified by 1:3 water model experiments. In these experiments, the water and blended oil (prepared by blending kerosene and vacuum pump oil with a certain ratio) on top of the water model are applied to represent the liquid steel and slag layer, respectively. The color of blended oil is transparent yellow that the movement can be easily captured by the camera during experiments.

The ratios of injection velocity and flow rate between real liquid metal and the water experiments can be calculated based on the equal Froude number (F_r):

$$F_{r_p} = F_{r_m}, \quad \frac{v_{\text{steel}}^2}{gL_{\text{steel}}} = \frac{v_{\text{water}}^2}{gL_{\text{water}}}, \quad [12]$$

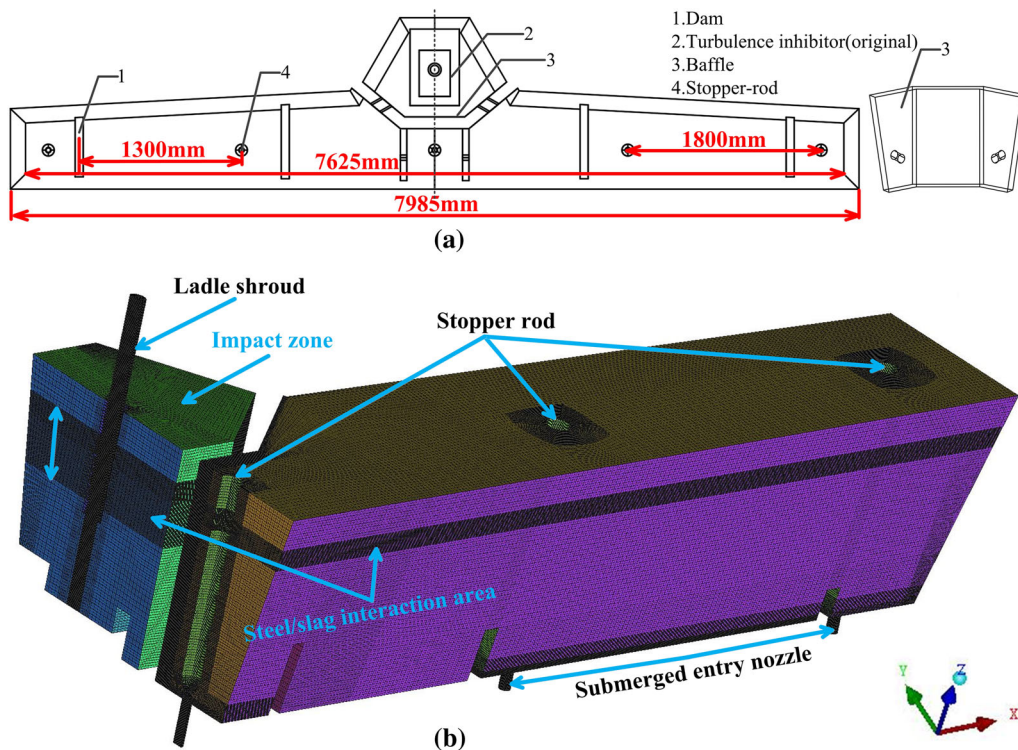


Fig. 2—Configuration of the tundish (a) and mesh distribution (b) of the computational model.

Table I. Main Industrial Parameters Applied in the Calculations

| Casting Condition | Value |
|---|-----------------------|
| Working Capacity of Tundish (t) | 35 |
| Bloom Cross Section (mm^2) | 280×380 |
| Casting Speed (m/min) | 0.63 |
| Steel Level at Steady State (mm) | 800 |
| Inner Diameter of Shroud (mm) | 81 |
| Submergence Depth of Shroud (mm) | 310 |
| Thickness of Slag Layer (mm) | 40 |
| Inner Diameter of SEN (mm) | 50 |
| Q_{steady} (m^3/s) | 2.66×10^{-3} |
| Velocity of Outlets (m/s) | 0.569 |

where F_{r_p} and F_{r_m} , v_{steel} and v_{water} , and L_{steel} and L_{water} , are the Froude number, velocity, and characteristic lengths in the real tundish and water model, respectively, and the scale factor $\lambda = \frac{L_{\text{water}}}{L_{\text{steel}}} = \frac{1}{3}$; then, the $v_{\text{water}} = \sqrt{\lambda}v_{\text{steel}}$, and the ladle throughput rate in the water model experiments $Q_{\text{water}} = \lambda^{\frac{5}{2}}Q_{\text{steel}}$ can be calculated.

Considering that the fluctuations of phase interfaces are mainly affected by interfacial tension, the Weber number between the real tundish and the water experiment should remain the same:

$$\begin{aligned} W_{e_p} &= W_{e_m} \cdot \frac{v_{\text{steel}}^2 \rho_{\text{steel}}}{[\sigma_{\text{steel-slag}} g (\rho_{\text{steel}} - \rho_{\text{slag}})]^{1/2}} \\ &= \frac{v_{\text{water}}^2 \rho_{\text{water}}}{[\sigma_{\text{water-oil}} g (\rho_{\text{water}} - \rho_{\text{oil}})]^{1/2}}. \end{aligned} \quad [13]$$

Then, the density of oil used in the water model experiments can be calculated by solving Eqs. [9] and [10]:

$$\rho_{\text{oil}} = \rho_{\text{water}} - \frac{v_{\text{water}}^4 \cdot \rho_{\text{water}}^2 \cdot \sigma_{\text{steel-slag}}^2 (\rho_{\text{steel}} - \rho_{\text{slag}})}{v_{\text{steel}}^4 \cdot \rho_{\text{steel}}^2 \cdot \sigma_{\text{water-oil}}^2}, \quad [14]$$

where W_{e_p} and W_{e_m} are the Weber numbers of the real tundish and the water model, respectively, and $\sigma_{\text{steel-slag}} = 1.6$ and $\sigma_{\text{water-oil}} = 7.3 \times 10^{-3}$ are the interfacial tension coefficients. The densities of pure kerosene and vacuum pump oil are 799 and 884 kg/m^3 , respectively. So, the ratio of kerosene and vacuum pump oil in the blended oil can be calculated by the value of ρ_{oil} .

A schematic diagram of the water model experiment system (a) and plexiglass model (b) in the laboratory is presented in Figure 3.

Figure 4 shows the comparison between the simulation and experimental results of slag entrapment at 0.9 seconds (a) and steel exposure in the impact zone at 12 seconds (b) during the filling process of the ladle changeover operation under the original turbulence inhibitor (rectangle), LS immersion depth (310 mm), ladle throughput rate ($2Q_{\text{steady}}$), and ladle changeover

time (3 minutes) conditions. In this experiment, the change in color of the slag phase represents volume fraction variations. Table II lists the comparisons between the numerical exposed area of steel (twice of the simulated result because half of the full-scale tundish was taken into account) in the impact zone and the measured experimental results (scaled up by the principle of similarity) under the same changeover conditions as in Figure 4 at different filling times. The exposed areas of molten steel in the experiments are calculated and measured by analyzing the photographs, and each measured result is obtained by averaging three groups of data under the same experimental conditions at the same filling time to ensure the reliability of experimental results. The simulated slag entrapment and steel exposure behavior are basically consistent with the results of the water model experiments, and compared to those obtained from the water model experiments, the simulated exposed areas of steel in the impact zone at different times have an error within 5 pct.

B. Effect of Technological Conditions

To investigate the effect of technological conditions on the multiphase flow behavior during ladle changeover process, according to Figure 1, the initial condition for the calculation of the ladle changeover process should be the flow and phase distribution status at steady-state casting. Figure 5 shows the velocity vector in the whole computational domain (a) and turbulent kinetics energy (TKE) distribution in the impact zone (b) at steady-state casting under the original technological conditions (ladle throughput rate is twice the injection rate at steady state, shroud immersion depth is 310 mm, structure of turbulence inhibitor is rectangular type without eave, and ladle changeover time is 3 minutes, respectively). It can be seen that the molten steel is injected from ladle to the impact zone with velocity of 1.2051 m/s at inlet through LS, impinges at tundish bottom, and splits into two upwards branches, then enters into the casting zone, finally flows into the mold through SEN. The maximum TKE in the impact zone is about $2.0 \times 10^{-2} \text{ m}^2/\text{s}^2$ and decreases to $2.1 \times 10^{-3} \text{ m}^2/\text{s}^2$ near the steel/slag interface, respectively, the remarkable TKE at steel/slag interface can easily cause level fluctuation and steel exposure.

After obtaining the stable steady-state field, then, changing the boundary condition for computational inlet from “velocity inlet” to “pressure inlet” (draining process during ladle changeover), when the next ladle arrives, the inlet boundary accordingly changes from “pressure inlet” to “velocity inlet,” and the velocity value should be calculated by the ladle throughput rate at refilling stage.

Formerly, the initial technological conditions for the five-strand bloom casting tundish during ladle changeover process were applied in the production, while the slag entrainment, large area, and duration of molten steel exposure usually occur during the ladle changeover period, and lead to a high disqualification rate of ultrasonic flaw detection in the steel rails. Therefore, it is

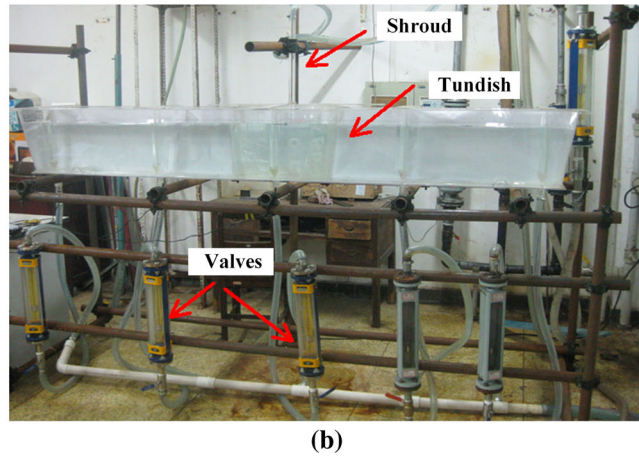
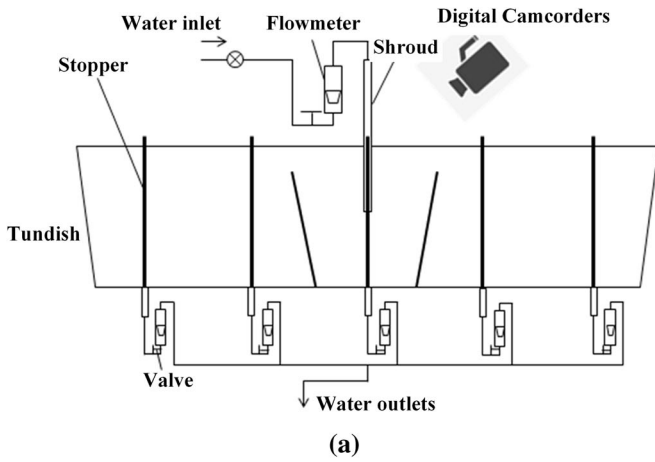


Fig. 3—Schematic diagram (a) and plexiglass model (b) for water experiments.

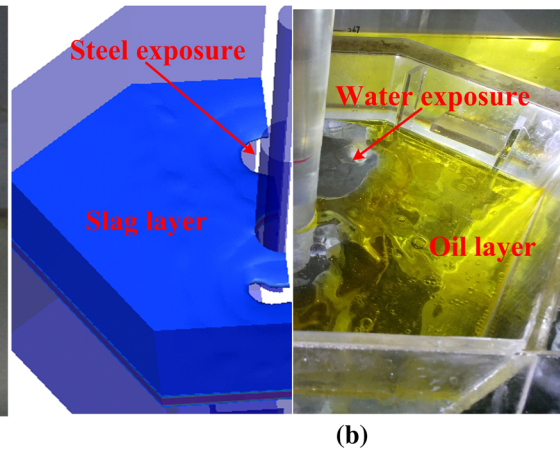
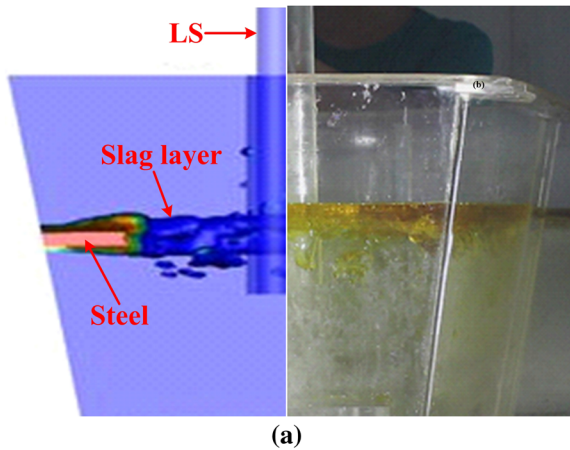


Fig. 4—Comparison of slag entrapment at 1.3 s (a) and steel exposure behavior at 12 s (b) between simulations and experiments.

Table II. Comparison of Numerical and Experimental Exposed Areas of Steel in the Impact Zone Under the Same Changeover Conditions as in Fig. 4

| | | | |
|--------------------------------|-----|-----|-----|
| Time (s) | 0.9 | 5.0 | 20 |
| Simulations (cm ²) | 167 | 205 | 175 |
| Experiments (cm ²) | 174 | 197 | 168 |
| Errors (Pct) | 4.2 | 4.1 | 4.2 |

necessary and significant to investigate the effect of ladle changeover conditions on the metallurgical behavior in the tundish during filling process of ladle changeover.

1. Ladle throughput rate of the Shroud

During the filling process (second stage of the ladle changeover process), the injection rate (Q) not only determines the rising speed of the molten steel level but also has a significant effect on the flow pattern of fluids in the tundish. The original injection rate is twice Q_{steady} (Figure 1). To investigate the exact effect of the injection rate on the flow pattern of the fluids and behavior of the steel–slag–air interfaces, the ladle changeover process

under injection rate values of $Q = 1.5Q_{\text{steady}}$, $Q = 2Q_{\text{steady}}$, and $Q = 3Q_{\text{steady}}$ are investigated and compared in this section, in which the ladle changeover time, shroud immersion depth, and turbulence inhibitor are 3 minutes, 310 mm, and rectangular type, respectively.

Figure 6 shows the variations in air in the molten steel with filling time under different injection rates on the basis of a constant outflow rate. The air injected into the impact zone of tundish by the injection flow is originally from the LS before the filling process. It can be seen that under ladle throughput rates of $Q = 1.5Q_{\text{steady}}$ and $Q = 2Q_{\text{steady}}$, the similar behavior of air in the molten steel in the impact zone is due to the injection flow from the shroud to the tundish at the early stage of the filling process. Moreover, most of the air in the shroud is expelled from the shroud (tundish) to the slag layer near the shroud as large bubbles within a short time due to the significant buoyancy force. When the ladle throughput rate increases to three times Q_{steady} , the air in the shroud is injected into the tundish by the molten steel with high velocity and is broken into a large number of small bubbles. The bubbles are distributed in many positions of the impact zone, and then the bubbles

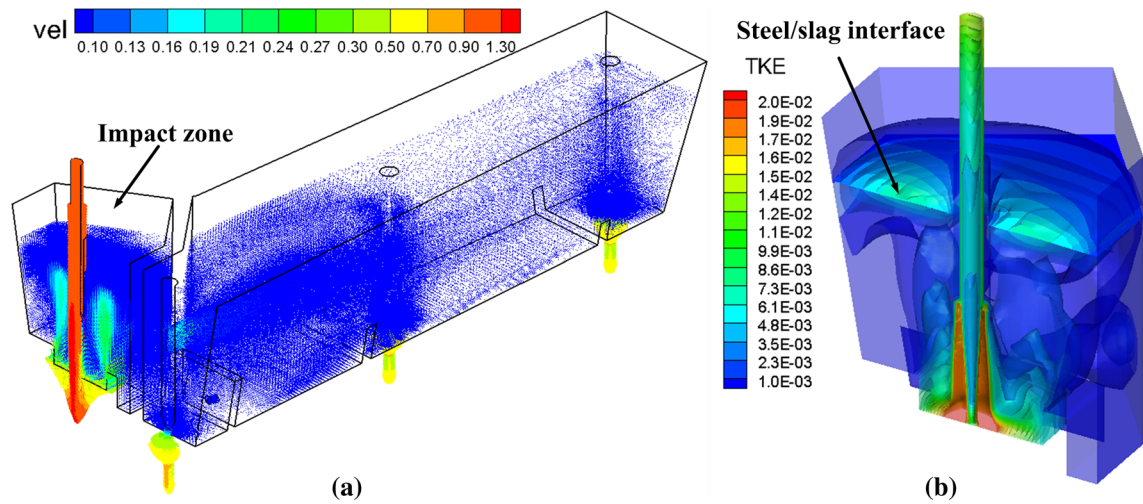


Fig. 5—Velocity vector in the tundish (a) and TKE in the impact zone (b) at steady-state casting.

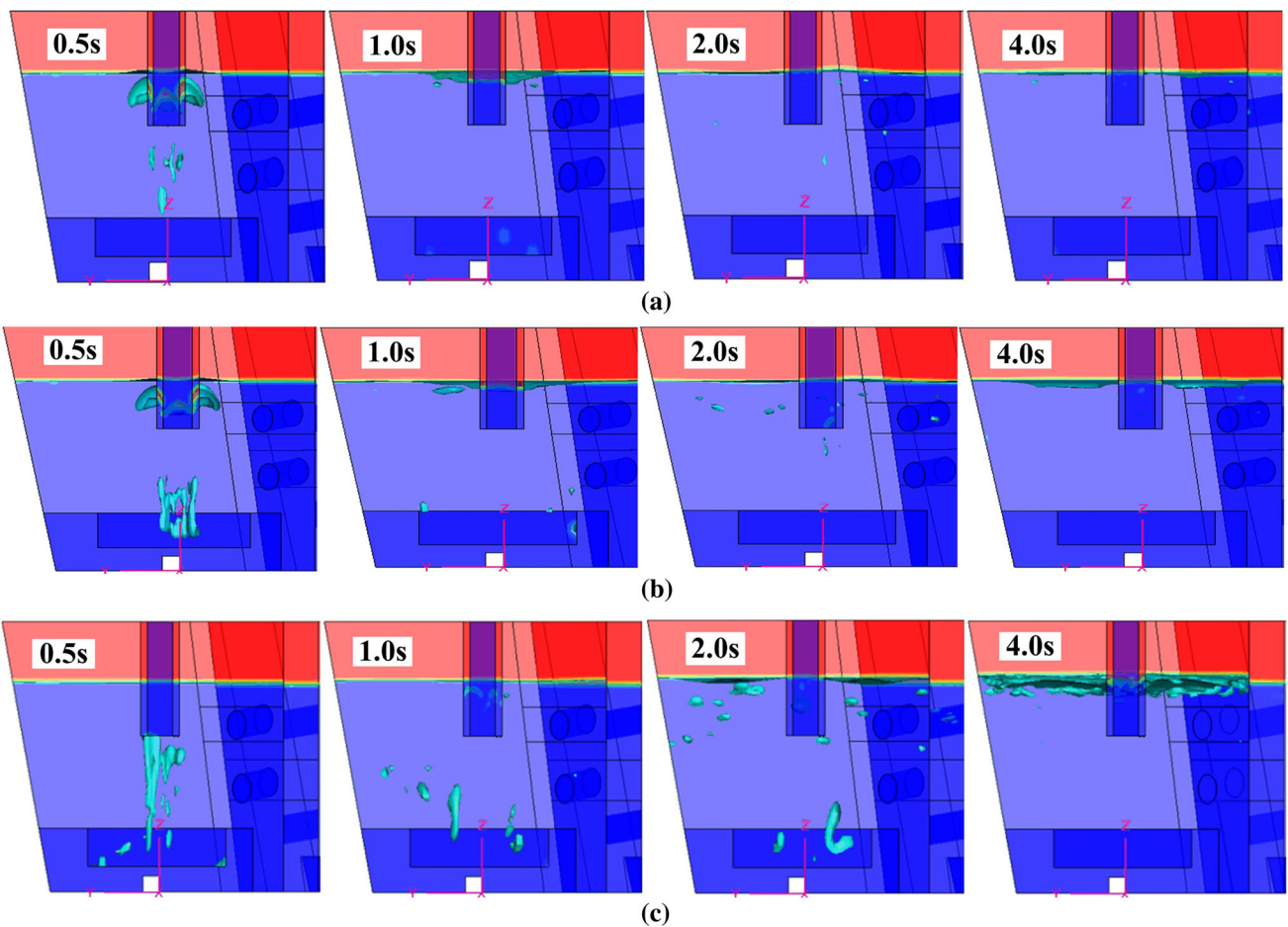


Fig. 6—Variations in air in the molten steel with filling time under different injection rates ((a) $Q = 1.5Q_{steady}$, (b) $Q = 2Q_{steady}$, (c) $Q = 3Q_{steady}$).

floating to the slag layer is not restricted to the area near the shroud. Moreover, some of the bubbles with smaller diameters cannot escape from the slag layer to the air in a short time due to the insufficient buoyancy drive and large interfacial tension.

Figure 7 shows schematic views of the slag layer in the impact zone under different ladle throughput rates when the filling time is 30 seconds. It is shown that the ladle throughput rate has a significant effect on the behaviors of the steel–slag–air interfaces. When the injection rate is

$1.5Q_{\text{steady}}$, the slag layer cannot be broken by the impact of the upper recirculation flow of the injection flow at the bottom of tundish. By contrast, significant breaking of the slag layer near the two sides of the shroud occurs when the injection rate increases to $2Q_{\text{steady}}$ and $3Q_{\text{steady}}$ because of the increase in flow intensity near the slag layer due to the huge impingement effect of the injection flow at the tundish bottom, and the exposed area of molten steel is increased as the ladle throughput rate is enhanced.

Figure 8 presents the variation in the exposed area of molten steel with filling time during the ladle changeover process under different ladle throughput rates. Figure 8(a) shows that at the early stage of the filling process (0 to 2 seconds), the maximum exposed area of molten steel is approximately 167 cm^2 at a filling time of 0.9 seconds when the ladle throughput rate is $1.5Q_{\text{steady}}$, while it decreases to 124 cm^2 at 0.8 seconds when the injection rate increases to $2Q_{\text{steady}}$. Furthermore, in the first two seconds, the exposed area of molten steel cannot be found when the injection rate is $3Q_{\text{steady}}$ because of the small bubbles formed due to the high injection velocity of molten steel and because of the crushing behavior of the small bubbles at the steel–slag interface, which cannot cause the slag layer to break. As the filling process continues (2 to 150 seconds), the slag layer cannot be broken when the injection rate is $1.5Q_{\text{steady}}$, while an obvious and similar variation trend in the exposed area can be found when the injection rates are $2Q_{\text{steady}}$ and $3Q_{\text{steady}}$. The magnitude of the exposed area is evidently larger when the injection rate is $3Q_{\text{steady}}$ than when the injection rate is $2Q_{\text{steady}}$ at the same filling time. When the injection rate is $3Q_{\text{steady}}$, the maximum exposed area of molten steel is 713 cm^2 at 2.5 seconds and remains over 570 cm^2 between 30 and

60 seconds. By contrast, the maximum exposed area of molten steel is 252 cm^2 at 4 seconds when the injection rate is $2Q_{\text{steady}}$ and remains at approximately 150 cm^2 between 30 and 60 seconds.

Overall, the ladle throughput rate has a significant effect on the multiphase flow pattern in the tundish during the filling process. A large area of molten steel exposed in the impact zone with a long filling time can be obtained when the ladle throughput rate is greater than $2Q_{\text{steady}}$, and the exposed area increases as the injection rate increases. However, the exposed area of molten steel in the impact zone can be nearly eliminated after 1.5 seconds when the ladle throughput rate is below $1.5Q_{\text{steady}}$.

2. Immersion depth of Shroud

The flow behavior in the tundish during the filling process under three immersion depths of 220 mm, 310 mm (original), and 400 mm is investigated in this section, in which the ladle changeover time, ladle throughput rate, and turbulence inhibitor are 3 minutes, $2Q_{\text{steady}}$, and rectangular type, respectively. Figure 9 shows the variations in steel fluctuations (a) and exposed area of molten steel (b) with filling time during the ladle changeover process under different shroud immersion depths. In this experiment, the ladle throughput rate is $2Q_{\text{steady}}$, and the level height of liquid steel at the beginning of the filling process is 650 mm.

Figure 9(a) shows that the value of steel level fluctuations in the impact zone rapidly increasing at the early stage of the filling process and reaches over 30 mm when the filling time is approximately 5 seconds. Then, a minor decrease occurs as the filling time increases. The level fluctuation decreases slightly as the immersion depth increases, and the maximum level fluctuation when

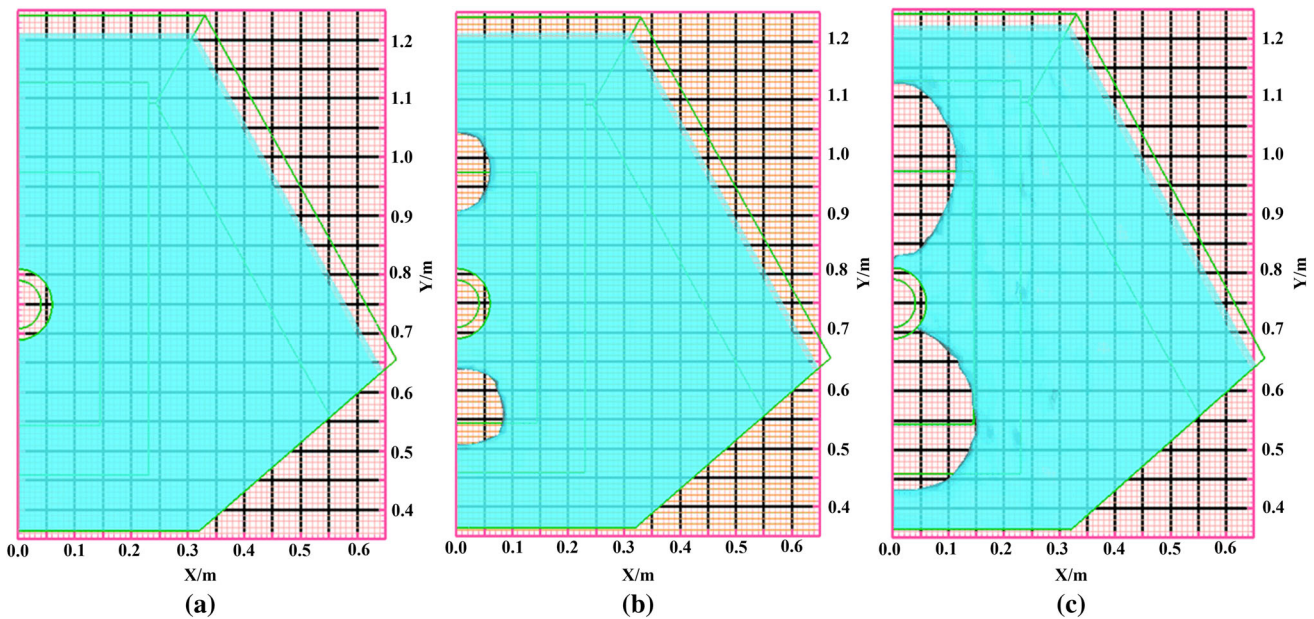


Fig. 7—Schematic views of the slag layer in the impact zone under different ladle throughput rates at 30 s ((a) $Q = 1.5Q_{\text{steady}}$, (b) $Q = 2Q_{\text{steady}}$, (c) $Q = 3Q_{\text{steady}}$).

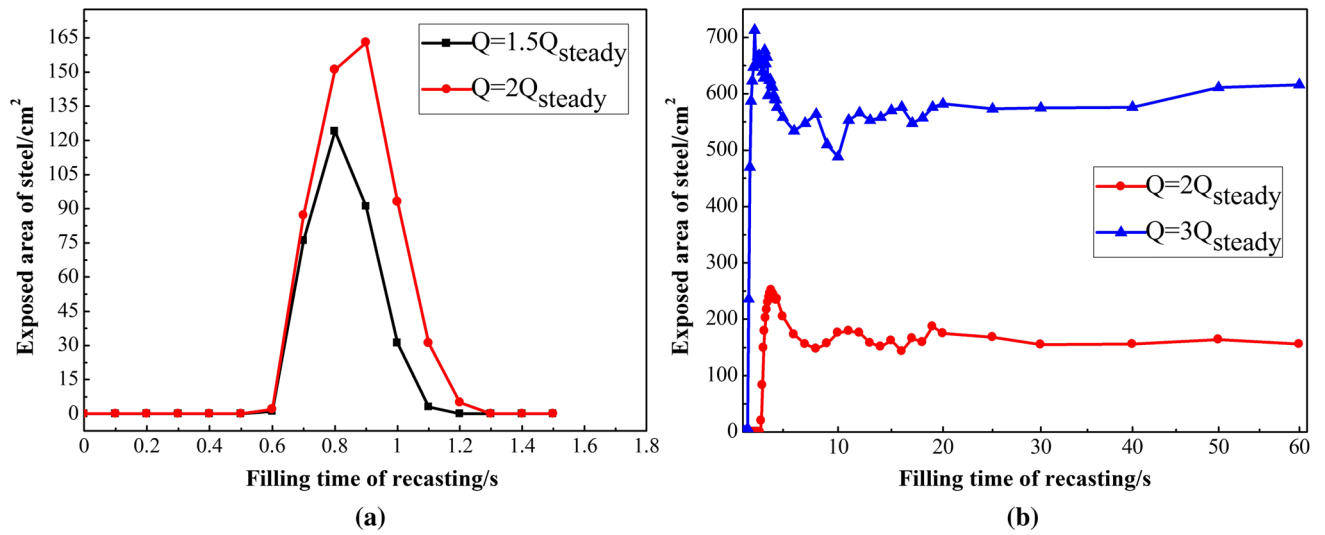


Fig. 8—Variation in exposed area with filling time under different ladle throughput rates ((a) 0 to 1.8 s, (b) 0 to 60 s).

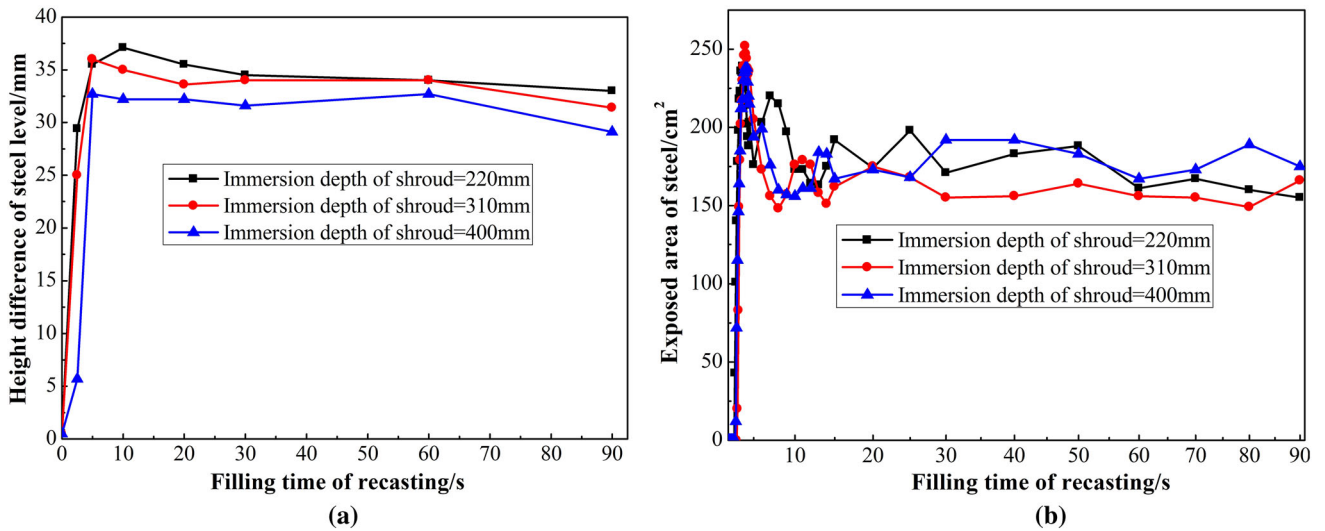


Fig. 9—Variations in steel fluctuations (a) and exposed area of molten steel (b) with filling time under different shroud immersion depths.

the immersion depth is 220 mm is approximately 37.1 mm, which is only approximately 4.9 mm higher than the case with an immersion depth of 400 mm.

In Figure 9(b), the exposed area of molten steel first decreases and then increases as the immersion depth of the shroud increases. The exposed area of molten steel from 30 to 90 seconds is relatively large when the immersion depth of the shroud is 400 mm and remains at approximately 170 cm², while the exposed area fluctuates around approximately 150 cm² when the immersion depth is 310 mm. Overall, compared to the ladle throughput rate, the immersion depth of the LS has less effect on the variation in the exposed area of molten steel in the tundish with filling time during the ladle changeover process, and the exposed area of molten steel undergoes a certain increase when the

immersion depth is too large or small. Therefore, the optimal shroud immersion depth in this situation should be approximately 310 mm.

3. Turbulence inhibitor

The turbulence inhibitor significantly affects the turbulent flow behavior in a continuous casting tundish in both the steady-state and transient-state processes, especially the flow pattern in the impact zone. The impact zone during the transient casting process in the tundish with the original turbulence inhibitor (see Figure 10(a), rectangular without eave) can easily cause slag entrapment and a large exposed area of molten steel in the impact zone. Therefore, the optimized structure of the turbulence inhibitor (see Figure 10(b), circular with

eave) and the detailed dimensions of the original and optimized turbulence inhibitor are presented in Figure 10.

Figure 11 shows the verification and comparison of injection flow trajectories at the early stage of the filling process between the original (a) and optimized (b) turbulence inhibitors, in which the ladle changeover time, shroud immersion depth, and ladle throughput rate are 3 minutes, 310 mm, and $2Q_{\text{steady}}$, respectively. This figure shows that the optimized turbulence inhibitor can clearly reduce the turbulence intensity near the free surface and that the turbulent flow model is suitable for simulating the turbulent behavior in the tundish. Figure 12 presents the distribution of TKE (a) and velocity vectors (b) at the free surface in the impact zone before and after optimization of the turbulence inhibitor. The optimized turbulence inhibitor can evidently decrease the turbulence intensity in

the impact zone, especially the maximum TKE at the free surface, which decreases from 2.5×10^{-3} to $5 \times 10^{-4} \text{ m}^2/\text{s}^2$. This decrease can significantly reduce the probability of slag entrapment in this area. Furthermore, the velocity at the free surface of the impact zone is nonuniformly distributed when using the original turbulence inhibitor. In this case, the maximum velocity is approximately 0.16 m/s and is distributed at two sides at the shroud, which may readily cause severe slag entrapment there. When the optimized turbulence inhibitor is applied, a relatively uniform distribution of velocity at the free surface in the impact zone can be obtained, and the maximum velocity decreases to 0.085 m/s. The turbulence inhibitor can clearly decrease the turbulence intensity in the impact zone, reduce the velocity of the free surface, then lessen the probability of slag entrapment, and decrease the exposed area of molten steel.

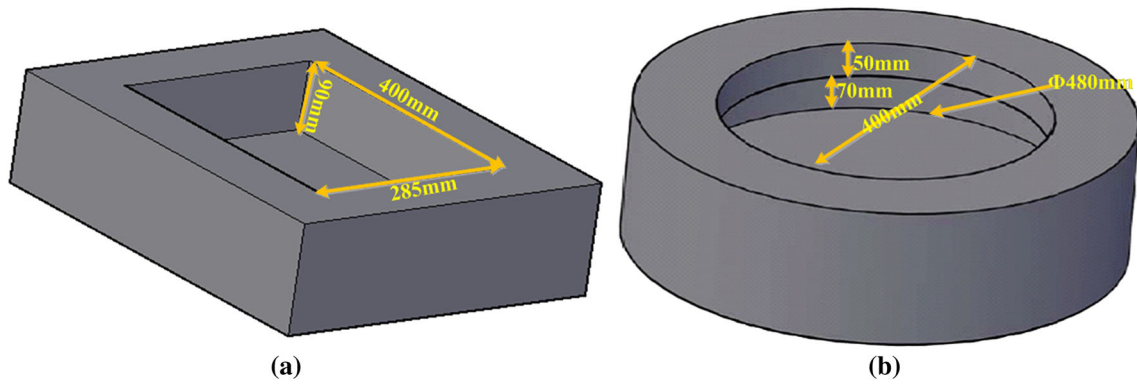


Fig. 10—Structure of the original (a) and optimized (b) turbulence inhibitor.

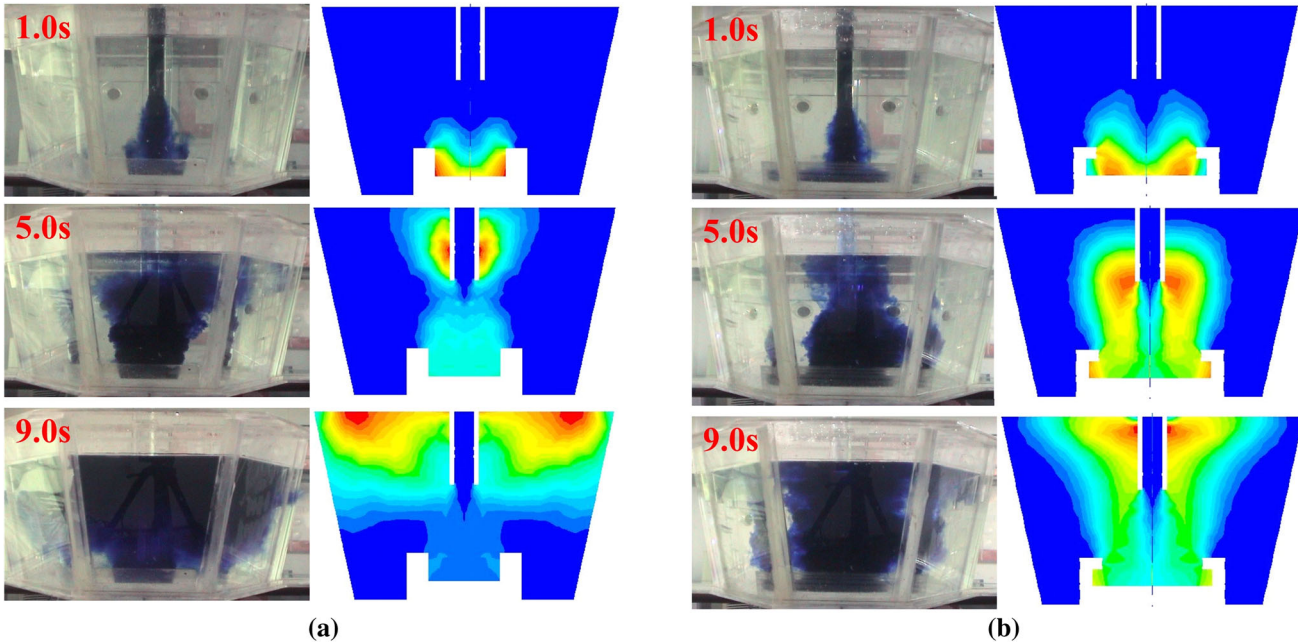


Fig. 11—Comparison of the injection trajectory at the early stage of the filling process between the original (a) and optimized (b) turbulence inhibitors.

Figure 13 shows the level heights of molten steel in the impact zone during ladle changeover at different x planes with the original (a) and optimized (b) turbulence inhibitor when the filling time is 5, 30, and 60 seconds. Figure 14 presents the simulated level fluctuation variations in the impact zone at the $x = 0$ plane with the filling time during ladle changeover before and after optimization of the turbulence inhibitor. As shown in Figure 13(a), two wave crests in the molten surface approximately 0.2 m away from the shroud (with Y coordinate is 0.75) in the impact zone can be observed, and the maximum level fluctuation happens at the symmetry plane ($x = 0$). As the plane moves forward along the x direction, the value of the level fluctuation gradually decreases, and the crests vanishes at the $x = 0.25$ m plane. Furthermore, the height of the steel level in the impact zone decreases as the filling time increases. Simultaneously, the area of the fluctuation region in the impact zone first increases and then decreases as the filling time increases.

When the optimized turbulence inhibitor is applied, the level fluctuations are scattered around the area near the shroud and decrease as the distance from the shroud center increases. Comparing the distributions of level fluctuations before and after optimization of the turbulence inhibitor reveals that with the optimized turbulence inhibitor, the level height in the impact zone is significantly smaller, and the maximum value of the level fluctuation is only approximately 14.1 mm, which is an approximately 60.8 pct decrease compared to the original turbulence inhibitor. Furthermore, the height of the level fluctuation in the stable period is decreased from an initial value of 33 mm to approximately 10 mm, and the two crests are formed by the rising flow due to the impact of injection flow on the turbulence inhibitor.

Consequently, the optimized turbulence inhibitor can clearly make the level fluctuation in the impact zone during the filling process uniform, effectively reduce the impingement effect of the rising flow on the slag layer, and help alleviate the exposure of molten steel and slag entrapment due to the large level fluctuation.

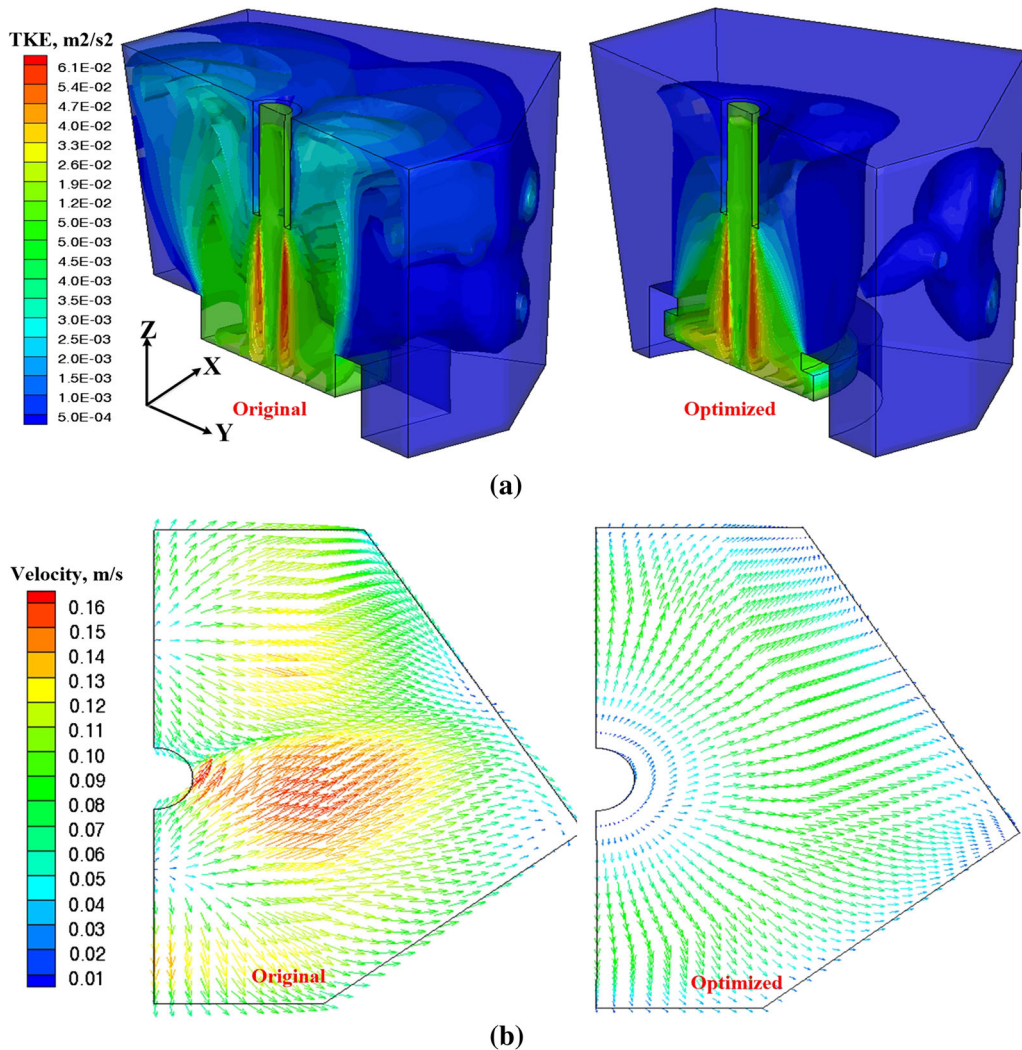


Fig. 12—The distribution of turbulent kinetic energy (TKE) (a) and velocity vectors (b) at the free surface in the impact zone before and after optimization of the turbulence inhibitor.

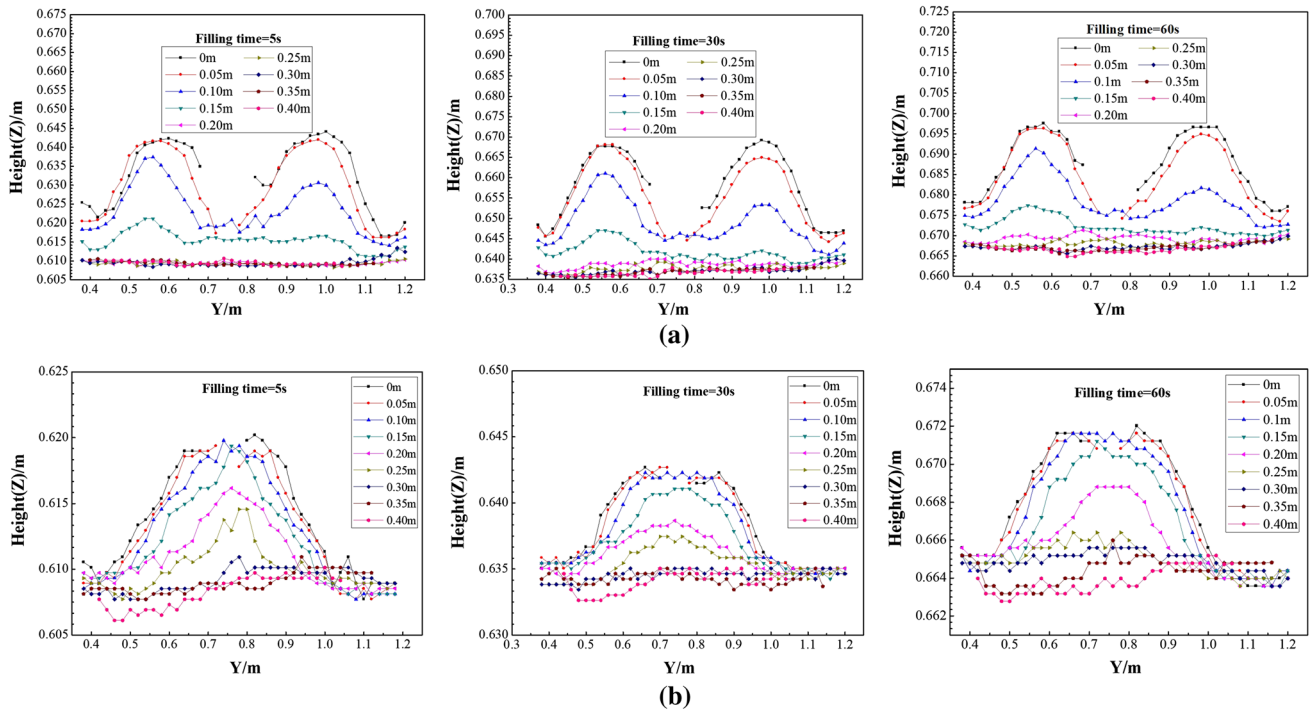


Fig. 13—The level heights in the impact zone during ladle changeover at different y - z planes with the original (a) and optimized (b) turbulence inhibitor.

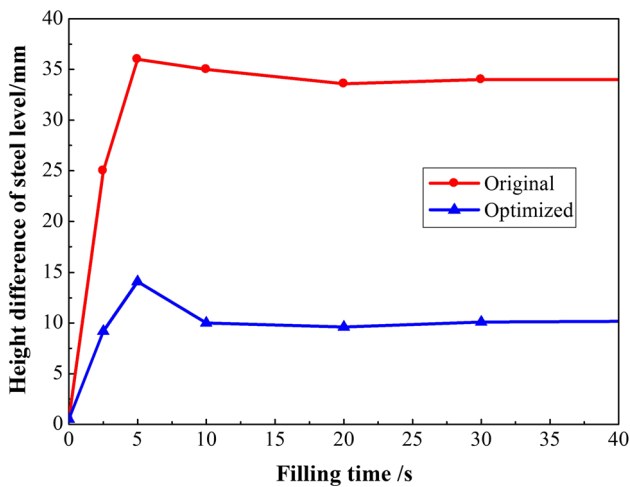


Fig. 14—Simulated level fluctuation variations in the impact zone at the $x = 0$ plane with the filling time using the original and optimized turbulence inhibitor.

4. Ladle changeover time

When the ladle changeover time is too large, the level of molten steel at the beginning of the filling process becomes too low, and the distance of the rising flow due to the impingement effect of the injection flow is apparently reduced, which can deteriorate the behavior of the steel-slag-air interfaces. As the original ladle changeover time is 3 minutes, to investigate the effect of changeover time on the flow behavior in the impact zone, the exposed area of molten steel and distribution of the slag layer under ladle changeover times of 2, 3,

and 4 minutes are investigated and compared, in which the ladle throughput rate, shroud immersion depth, and turbulence inhibitor are $2Q_{\text{steady}}$, 310 mm, and rectangular type, respectively. Figure 15 shows the variations of steel level height with empty time (a) and exposed area with filling time (b) under different ladle changeover times. Figure 16 presents the distributions of the slag layer in the tundish at a filling time of 5.0 seconds under different ladle changeover times.

Figure 15(b) shows that the heights of steel level at the beginning of refilling process are 705 mm for 2 minutes, 655 mm for 3 minutes, and 605 mm for 4 minutes, respectively. Then, the minimum distance of separation between steel level and shroud bottom for each emptying time are 215 mm for 2 minutes, 165 mm for 3 minutes, and 115 mm for 4 minutes, respectively. And the height of steel level gradually increases during the refilling process at the same speed as the descent speed when ladle throughput rate is $2Q_{\text{steady}}$. Figure 15(b) shows that the variations in the exposed area of molten steel with filling time under ladle changeover times of 2 and 3 minutes are basically consistent with each other, while the value of the exposed area is relatively small when the ladle changeover time is 2 minutes. The exposed area undergoes little change when the ladle changeover time is within 2 to 3 minutes. However, there is a significant change in the exposed area of molten steel in the impact zone when the ladle changeover time is 4 minutes, and a long ladle changeover time means a low steel level in the tundish at the beginning of the filling process. Therefore, a sharp increase in the exposed area of molten steel can occur during the first 5 seconds of the filling process, and a rapid increase

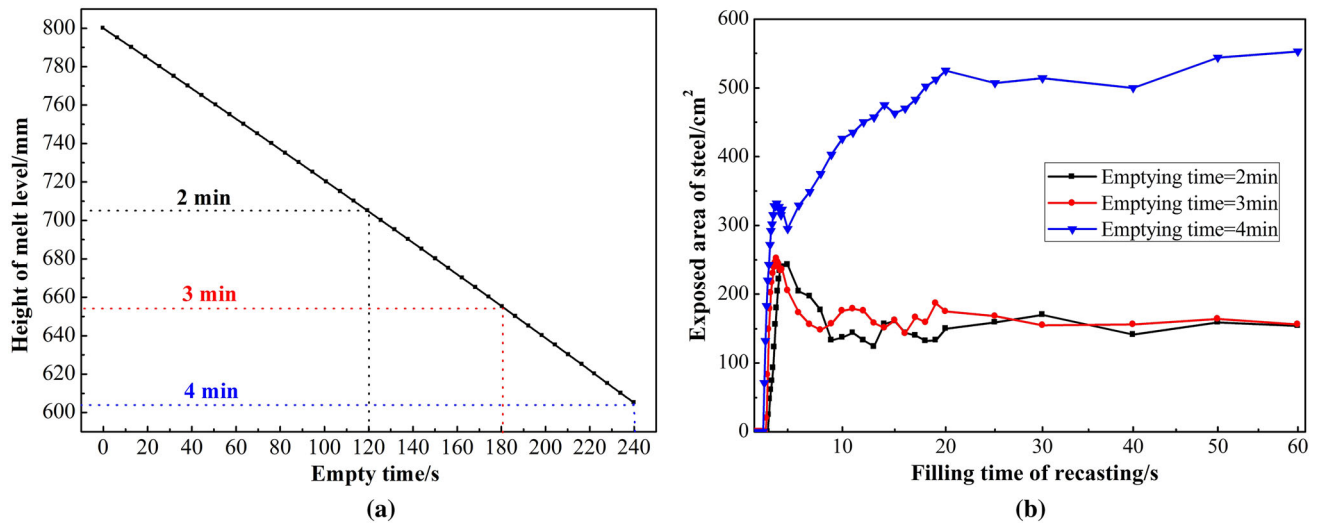


Fig. 15—Variations of steel level height with empty time (a) and exposed area with filling time (b) under different ladle changeover times.

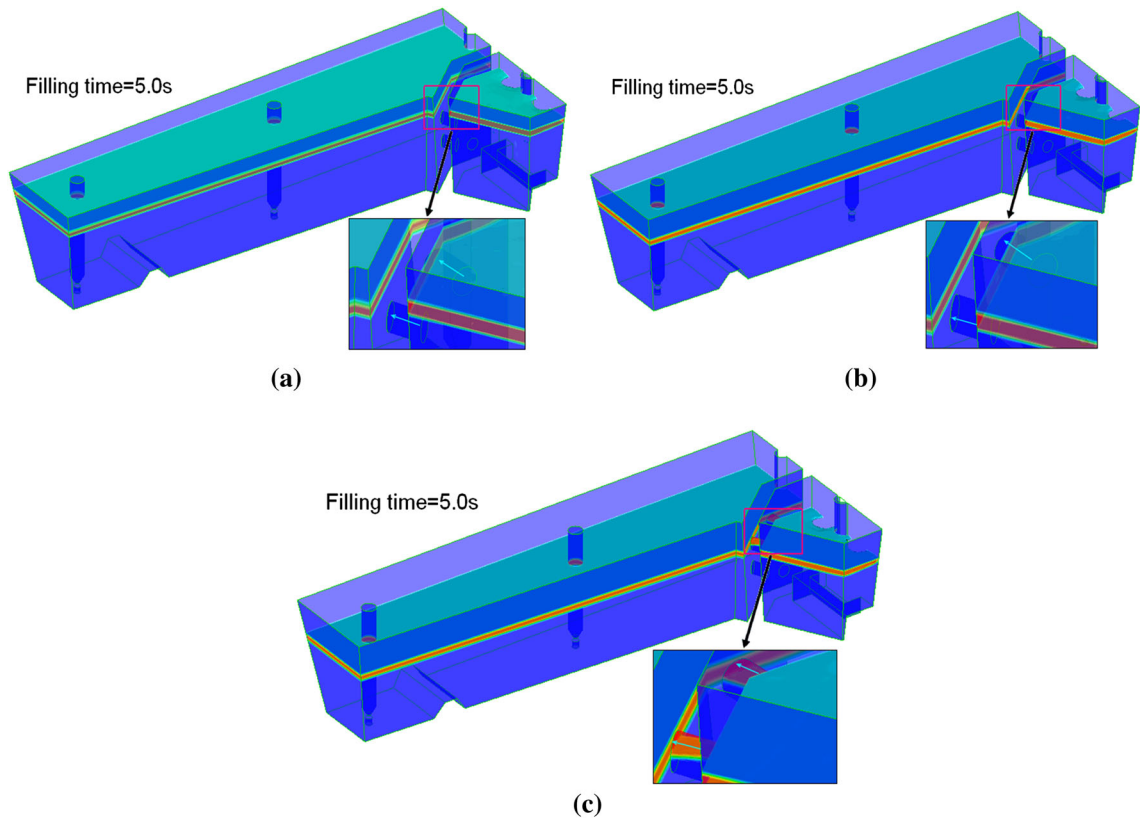


Fig. 16—Distribution of slag layer in the tundish under different ladle changeover times ((a) 2 min, (b) 3 min, (c) 4 min).

happens between 5 and 20 seconds of filling time. Moreover, the exposed area is relatively stable when the filling time is over 20 seconds, remaining at over 500 cm², which is far greater than the exposed area of molten steel in the impact zone after a filling time of 20 seconds when the ladle changeover time is 2 or 3 minutes. When the ladle changeover time is over 3 minutes, the flow behavior in the impact zone during

the filling process can be strongly affected as the ladle changeover time is extended, which can deteriorate the behaviors of the steel–slag–air interfaces and expand the exposed area of molten steel.

As shown in Figure 16, as the ladle changeover time increases, the height of the steel level drops during the emptying process. In particular, some of the covering slag in the impact zone enters the casting zone through

Table III. Comparison of FD Qualification Before and After Optimization of Ladle Changeover Conditions in Industrial Trials

| Ladle Changeover Condition | Number of Steel Rails | Disqualification Number of FD | Qualification Rate of FD (Pct) | FD Disqualification Caused by Ladle Changeover | FD Disqualification Rate Caused by Ladle Changeover (Pct) |
|----------------------------|-----------------------|-------------------------------|--------------------------------|--|---|
| Before Optimizations | 28,850 | 368 | 98.7 | 161 | 43.8 |
| After Optimizations | 29,724 | 267 | 99.1 | 69 | 25.8 |

the deflector holes when the ladle changeover time is 4 minutes, which may readily cause slag entrapment and reduce the purity of the steel in the tundish (see Figure 16(c)).

According to the above results, the ladle changeover time should be controlled within 3 minutes. The exposed area of molten steel in the impact zone during the filling process evidently increases when the ladle changeover time is over 4 minutes, which may cause some of the slag in the impact zone to float into the casting zone, aggravate slag entrapment, and reduce the cleanliness of the liquid steel in the tundish.

IV. APPLICATION EFFECT

According to the abovementioned results, the ladle changeover condition for the five-strand bloom casting tundish was improved as follows:

1. The opening percentage of the slide gate is 60 pct at the beginning of the filling process and then increases to 100 pct when there is no obvious splash in the impact zone. The filling process is quickly completed, and the automatic control system is turned on.
2. The ladle changeover time is strictly controlled within 3 minutes and should be as short as possible.
3. The circular turbulence inhibitor with eave (TI-B) is applied, and the immersion depth of the LS should be 310 mm.

The optimized ladle changeover conditions were applied in industrial trials for three months, and the qualification rates of flaw detection (FD) in the produced steel rails in the three months before and after optimization were compared. The comparative results are listed in Table III.

As shown in Table III, the qualification rate of FD in the steel rails is increased from 98.7 to 99.1 pct after applying the optimized conditions. Moreover, the flaw detection disqualification rate caused by ladle changeover operation is decreased from 43.8 to 25.8 pct of the total disqualified steel rails.

V. CONCLUSIONS

In this paper, the transient three-phase flow behavior in a five-strand bloom casting tundish during the ladle changeover process was numerically investigated, and the effect of ladle throughput rate, shroud immersion depth, turbulence inhibitor structure, and ladle

changeover time on the turbulent flow and level fluctuations during the filling process were analyzed to optimize the flow pattern in the tundish during ladle changeover. The conclusions of the investigations can be summarized as follows:

1. The exposed area of molten steel in the impact zone increases as the ladle throughput rate increases during the filling process. As the ladle changeover time is fixed at 3 minutes, the maximum exposed area is 713 cm² when the ladle throughput rate is $3Q_{\text{steady}}$, which is approximately 2.82 times than when the ladle throughput rate is $2Q_{\text{steady}}$. The exposure of molten steel in the impact zone can be eliminated when the ladle throughput rate is $1.5Q_{\text{steady}}$.
2. As the immersion depth of the shroud increases, a slight deterioration in the level fluctuation happens, while the exposed area of molten steel in the impact zone first decreases and then increases. The optimal immersion depth is 310 mm.
3. When the optimized turbulence inhibitor is applied, the two wave crests around two sides of the shroud vanish, the height of the level fluctuations is reduced, and the maximum level fluctuation during the stable period can be decreased from 33 mm to approximately 10 mm. Furthermore, the exposure of molten steel in the impact zone can be eliminated.
4. When the ladle changeover time is 4 min, the exposed area of molten steel in the stable period remains at over 500 cm², which is far more than the exposed area of 150 or 170 cm² when the ladle changeover time is 2 or 3 minutes, respectively. Additionally, some of the slag may enter the casting zone during the filling process due to the extremely low level of molten steel. The ladle changeover time should be controlled within 3 minutes.
5. The qualification rate of FD in the steel rails is increased from 98.7 to 99.1 pct after applying the optimized ladle changeover conditions, and the disqualification rate induced by ladle changeover is decreased from 43.8 to 25.8 pct.

ACKNOWLEDGMENT

The authors would like to express their gratitude for the financial support provided by the National Natural Science Foundation of China (51774217 and 51604201) and the Research Project of Hubei Provincial Department of Education (D20171104).

REFERENCES

1. K. Chattopadhyay, M. Isac, and R.I.L. Guthrie: *ISIJ Int.*, 2010, vol. 50, pp. 331–48.
2. Y. Sahai: *Metall. Mater. Trans. B*, 2016, vol. 47B, pp. 2095–2106.
3. S. Chatterjee, D. Li, and K. Chattopadhyay: *Metall. Mater. Trans. B*, 2018, vol. 49B, pp. 756–66.
4. A. Vakhrushev, M. Wu, A. Ludwig, G. Nitzl, Y. Tang, G. Hackl, and R. Wincor: *Steel Res. Int.*, 2017, vol. 88, p. 1600276.
5. A. Cwudziński: *Int. J. Cast Metals Res.*, 2017, vol. 30, pp. 50–60.
6. J. Zhang, S. Yang, M. Li, Z. Chen, Z. Jiang, and J. Li: *Ironmak. Steelmak.*, 2017, vol. 44, pp. 732–38.
7. R. Bölling, H. Odenthal, and H. Pfeifer: *Steel Res. Int.*, 2005, vol. 76, pp. 71–80.
8. J.M.F. Oro, C.S. Morros, J.R. Somoano, and M.A. Ordieres: *ASME fluids Engineering Division Summer Meeting*, 2009, pp. 2183–94.
9. M.I.H. Siddiqui and P.K. Jha: *Steel Res. Int.*, 2016, vol. 87, pp. 733–44.
10. S. Kant, P.K. Jha, and P. Kumar: *Ironmak. Steelmak.*, 2011, vol. 38, pp. 391–97.
11. K. Takahashi, M. Ando, and T. Ishii: *ISIJ Int.*, 2014, vol. 54, pp. 304–10.
12. H. Ling, L. Zhang, and H. Li: *Metall. Mater. Trans. B*, 2016, vol. 47B, pp. 2991–3012.
13. H. Ling, L. Zhang, and H. Wang: *Metall. Res. Technol.*, 2017, vol. 114, p. 516.
14. H. Ling and L. Zhang: *JOM*, 2013, vol. 65, pp. 1155–63.
15. S. Garcia-Hernandez, R.D. Morales, D.J.B. Jose, I. Calderon-Ramos, and E. Gutierrez: *Steel Res. Int.*, 2016, vol. 87, pp. 1154–67.
16. R.D. Morales, S. Garcia-Hernandez, J.D.J. Barreto, A. Ceballos-Huerta, I. Calderon-Ramos, and E. Gutierrez: *Metall. Mater. Trans. B*, 2016, vol. 47B, pp. 2595–2606.
17. M.M. Machado-Lopez, J.A. Ramos-Banderas, E. Torres-Alonso, J.J. Barreto, and S. Garcia-Hernandez: *Ironmak. Steelmak.*, 2013, vol. 40, pp. 326–34.
18. ANSYS Fluent 15.0 *Theory Guide*, Southpointe, 2013.

Publisher's Note Springer Nature remains neutral with regard to jurisdictional claims in published maps and institutional affiliations.